



HAL
open science

Dielectric characterization of $[\text{Fe}(\text{NH}_2\text{-trz})_3]\text{Br}_2\text{H}_2\text{O}$ thermal spin crossover compound by terahertz time domain spectroscopy

Patrick Mounaix, Noëlle Lascoux, Jérôme Degert, Eric Freysz, A. Kobayashi, Nathalie Daro, Jean-François Létard

► To cite this version:

Patrick Mounaix, Noëlle Lascoux, Jérôme Degert, Eric Freysz, A. Kobayashi, et al.. Dielectric characterization of $[\text{Fe}(\text{NH}_2\text{-trz})_3]\text{Br}_2\text{H}_2\text{O}$ thermal spin crossover compound by terahertz time domain spectroscopy. *Applied Physics Letters*, 2005, vol. 87, n° 24, 244103 (3 p.). 10.1063/1.2143123 . hal-00019143

HAL Id: hal-00019143

<https://hal.science/hal-00019143>

Submitted on 9 Feb 2022

HAL is a multi-disciplinary open access archive for the deposit and dissemination of scientific research documents, whether they are published or not. The documents may come from teaching and research institutions in France or abroad, or from public or private research centers.

L'archive ouverte pluridisciplinaire **HAL**, est destinée au dépôt et à la diffusion de documents scientifiques de niveau recherche, publiés ou non, émanant des établissements d'enseignement et de recherche français ou étrangers, des laboratoires publics ou privés.

Dielectric characterization of $[\text{Fe}(\text{NH}_2\text{-trz})_3]\text{Br}_2\cdot\text{H}_2\text{O}$ thermal spin crossover compound by terahertz time domain spectroscopy

P. Mounaix,^{a)} N. Lascoux, J. Degert, and E. Freysz

Centre de Physique Moléculaire Optique et Hertzienne, UMR CNRS 5798, Université Bordeaux I, 351 Cours de la Libération, 33405 Talence cedex, France

A. Kobayashi, N. Daro, and J.-F. Létard

Institut de Chimie de la Matière Condensée de Bordeaux (ICMCB), CNRS UPR 9048, Université Bordeaux I, Groupe des Sciences Moléculaires, 87 Avenue du Docteur Schweitzer, 33608 Pessac cedex, France

(Received 26 July 2005; accepted 17 October 2005; published online 8 December 2005)

The complex optical index refraction of an iron (II) spin-crossover coordination polymer is measured in the Terahertz frequency range by Terahertz time-domain spectroscopy (THz-TDS). By scanning the temperature from 288 to 333 K, we have recorded the evolution of the THz spectrum within the low spin - high spin thermal hysteresis loop. We were able to simultaneously infer the refractive index and absorption variations. The low spin-high spin transition has a marked spectral signature in the millimeter wavelength. In the 0.1–0.6 THz frequency range, the variation of real and imaginary part of the index of refraction is 6% and 20%, respectively. A marked absorption is observed above 500 GHz. The THz-TDS provides a clear direct fingerprint of this class of materials, which are interestingly potential candidates for optical data storage and processing devices. © 2005 American Institute of Physics. [DOI: 10.1063/1.2143123]

The ability of spin crossover (SCO) materials to change their magnetic, structural, and optical properties stimulated by pressure, temperature, or light has led to increasing interest.¹ Their potential use in technological applications such as molecular switches, data displays, data storage devices, and more recently as intelligent contrast agents for magnetic resonance imaging are particularly important.^{2–4}

In this context, one of the most promising example is certainly offered by iron (II) SCO materials, which exhibit a change of the spin state from a paramagnetic high spin state (HS, $S=2$) to a diamagnetic low spin state (LS, $S=0$). In some peculiar conditions, when the interaction between the metal center is strong, as in the case of polymeric coordination iron (II) complexes, the spin state modification on a macroscopic scale is a first-order phase transition accompanied by a thermal hysteresis behavior and the given material possesses a memory property to the compounds.² In fact, the phase transition results in a drastic change of numerous properties of the material, such as the absorption spectrum, the magnetic response and the dielectric constant for example. However, to clearly foresee the potential industrial developments of these compounds, it is necessary to qualitatively and quantitatively characterize the optical and dielectric properties. In this situation, noninvasive methods such as optical and spectroscopic techniques are of particular interest, especially in the far infrared where collective behaviors are revealed. For instance, one may wonder how these promising compounds could behave in the 0.1–2 THz spectral range. Terahertz technique has undergone remarkable development in, e.g., THz imaging,^{5,6} biomedical media analysis,^{7,8} and time domain far-infrared spectroscopy.⁹ Furthermore, time resolved experiments are now mature with optical pump-terahertz probe spectroscopy.^{10–13} Unfortunately, most of the optical properties of SCO materials in the

far infrared region are still missing and deserve further analysis. Our main motivation is then to supply experimental data at Terahertz wavelengths.

In this article, we fully characterize the optical constants in the THz range of a well-known iron (II) complex, the $[\text{Fe}(\text{NH}_2\text{-trz})_3]\text{Br}_2\cdot\text{H}_2\text{O}$ with $\text{NH}_2\text{-trz}=1,2,4\text{-aminotriazole}$, which displays a thermal hysteresis at room temperature.¹⁴ The Terahertz time domain spectroscopy experiment can be used to demonstrate that the evolution of the molecular spin transition can be followed recording the real and imaginary part of the refraction index within the hysteresis loop in the 0.1–2 THz frequency range.^{15–17}

To carry the THz experiments, we have selected the $[\text{Fe}(\text{NH}_2\text{-trz})_3]\text{Br}_2\cdot\text{H}_2\text{O}$ complex. The synthesis and spin-crossover properties have been already published.^{14,18} In Fig. 1(a) we report the evolution of the reflectivity signal recorded at 530 ± 50 nm which shows the thermal spin transition at $T_{1/2\downarrow}=294$ K on the cooling mode and at $T_{1/2\uparrow}=313$ K on the warming mode. It presents a hysteresis loop of 20 K at room temperature. This complex, in powder form, is then inserted for the THz experiments in a 2 mm thick quartz cell. A microscopic analysis of the powder showed that the typical area of the particles is few μm^2 . The cell temperature is monitored and controlled using a Shimaden SR 25 proportional integral differential (PID) controller which has a temperature stability of ~ 100 mK.¹⁵ Finally, the sample is mounted on a three-dimensional (3D) stage and precisely placed into the THz interaction region and we have also checked the invariable dielectric response of the sample while translating the interaction area along the tested cell. To subtract the contribution of the empty cell, we measured its index by THz-TDS on the 294–333 K temperature range. It was found constant in the whole temperature range.

Figure 2 shows a series of averaged time domain spectra obtained at different temperatures of the sample on the cooling and warming mode. On this figure, we have also reported the large THz reference signal measured when the cell is

^{a)} Author to whom correspondence should be addressed; electronic mail: p.mounaix@cpmoh.u-bordeaux1.fr

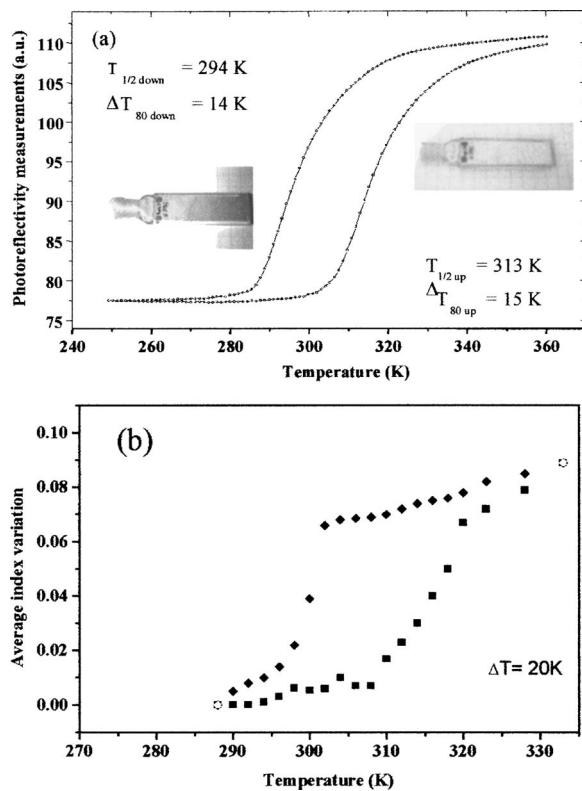


FIG. 1. (a) Thermal hysteresis loop detected optically by following the change of the reflectivity spectra at 530 ± 50 nm. (b) Experimental data measured by THZ-TDS at 300 GHz.

removed. Data reported have a shifted coordinate for clarity purpose. The measurements were performed varying the temperature by 0.5 K. We clearly observe a positive or negative temporal phase shift when the sample is warmed or cooled, respectively. As shown on Fig. 1(a) known for this iron (II) complex, a drastic change of the color occurs with the change of the temperature. When the cell is heated in such way that all iron (II) metal ions behave into the HS electronic configuration and the sample is white, while at low temperature, i.e., in the LS situation, the material is pink.

The THz detection system we used makes it possible to measure the temporal profile of the electric field of the THz pulses and, therefore, to recover the complex index of refraction of the studied sample on a 0.1–2 THz range. The method implies to perform two measurements. We first record a reference waveform $E_{\text{ref}}(t)$ without the sample and then a signal

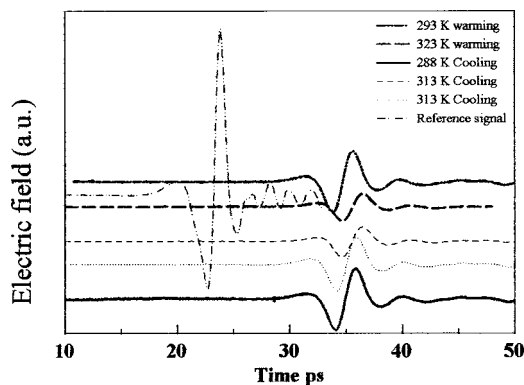


FIG. 2. Measured temporal spectra of original THz wave form and transmitted THz wave form through the cell at different temperature 293 and 323 K.

waveform $E_s(t)$ with the sample. The Fourier components of the two signals are obtained through a fast Fourier transform (FFT) and define the complex transmission function of the sample:

$$T(\omega) = \frac{E_s(\omega)}{E_{\text{ref}}(\omega)}. \quad (1)$$

In the case of a homogeneous sample, the complex refractive index $N = n + i\kappa$ is related to the complex transmission function provided. The frequency-dependent complex dielectric constant of the sample is obtained by computing the complex ratio of the output amplitude spectrum to the input of the reference spectrum. In fact, a major advantage of this technique is that it does not require performing any Kramers-Kronig analysis. Indeed, the experiment by itself gives direct access to the frequency characteristics of the electric field (amplitude and phase). The internal reflections of the sample are taken into account in the analytical expression of the transfer function, which is then numerically solved. This problem constitutes two equations for the real parameters n and κ . As a result, one obtains without any ambiguity¹⁹ the complex dielectric function of the sample in the entire spectral range transmitted by the THz pulse. The refractive index n mainly depends on the phase of the transmission function and was principally deduced from the phase shift due to the propagation of THz radiation. Hence the calculated refractive index is strongly affected by unavoidable errors in the determination of the cell thickness and refractive index. However, as the phase of the electric field is measured with a high accuracy, the absolute value of n can be precisely determined. Typically, the maximum uncertainty in optical data extraction is evaluated to be about 5% for an error of 10% in the sample thickness.²⁰

Figure 3 shows the Fourier transformed amplitude of the THz pulse with and without the sample at room temperature. These data indicate the maximum THz frequency range covered by our setup (around 2 THz) and clearly reveal the qualitative absorption of the studied sample in the THz range. Though we were aware that water vapor has a well-known spectrum fingerprint (i.e., the clear spectral dip in the reference signal in Fig. 3), which is due to 1.3 m free air propagation of the THz beam. However, our apparatus can be easily enclosed in water free environment. In Fig. 3, one can easily note that a strong absorption in the studied sample occurs in the sample between 500 GHz and 2 THz. Then the water absorption influence during the air propagation is minor. The maximum of the transmission is around 220 GHz. The straightforward conclusion is that this sample can be used as a stop-band material in the high THz frequency

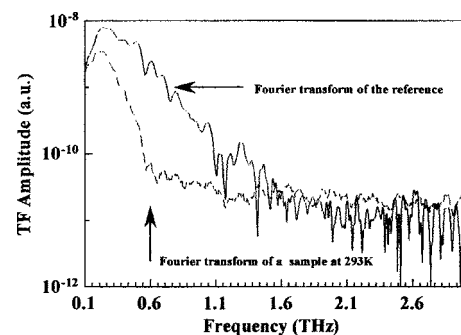


FIG. 3. Fourier transform of reference and sample signals.

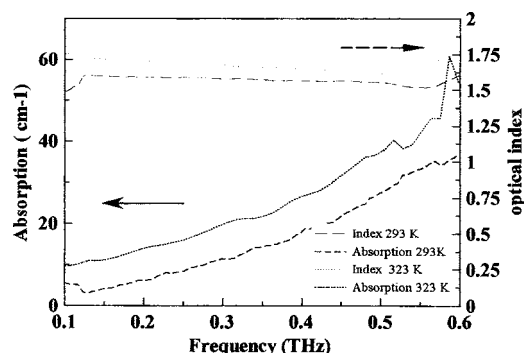


FIG. 4. Index and absorption data at 293 and 323 K.

range. However, our data raise number of important problems regarding, for instance, the mechanisms responsible for the high absorption coefficient of these samples. They will be discussed and published elsewhere. Let us now focus our attention on the properties of the complex in the low THz frequency range. In Fig. 4, we have reported the evolution of the optical index between 0.1 and 0.6 THz. At room temperature, the real part of the index of refraction is almost monotonous and is about $n=1.57$. We have checked that the index is almost constant in the whole cell and does not depend on the position of the THz pulse within the cell. In Fig. 4, we also report the evolution of the absorption coefficient in the HS state ($T=293$ K) and LS state ($T=323$ K) between 100 and 600 GHz. The maximum index change $\Delta n \sim 0.09$ corresponds to $\Delta n/n \sim 6\%$ index variation. This very high distinguishable variation along the entire bandwidth is a welcome feature for optical applications of this polymer. Concerning the absorption variation, we found that the absorption coefficient α evolves as $f^{1.8}$ where f is the frequency. In agreement with other reported data,²¹ this almost quadratic variation may reflect the superposition of many Lorentzian tails of several strong atomic oscillators well below resonant frequency (data are given for $f < 600$ GHz).

Finally in Fig. 1(b), we show the evolution of $\Delta n = \Delta n_S(T) - \Delta n_{LS}$ (the difference of the optical index of the sample n_S at T investigated high state minus the optical index in LS) as a function of the temperature for 220 GHz. This frequency corresponds to the largest THz electric field transmitted by the sample. The data uncertainties are evaluated to be ± 0.002 . Beside its slightly larger amplitude, the Δn variations in the THz range follow the reflectivity changes recorded in the visible [Fig. 1(a)] with a thermal hysteresis about 20 K wide. Moreover and as expected, we note that the temperature width of the hysteresis loop is independent of the scanned frequency range. The origin of these variations of the dielectric function of SCO compounds is supposed to result from the spontaneous distortion of the coordination sphere of the metal center. In fact, upon the spin crossover phenomenon, an important variation of the metal-ligand bond lengths occurs. It is induced by the deformation of the electronic molecular orbital between the LS and HS states. Therefore, the local electrical dipoles in the material must be different in both spin states, leading to a meaningful change in the permittivity of the material upon spin crossover.²²

In conclusion, we have shown that the THz-TDs technique can be efficiently used to quantitatively characterize the far infrared refractive index variations of SCO compounds. From the fundamental point of view, this dielectric hysteresis property is actually the first effective means indicating the potential use of spin crossover materials in electronic devices up to 500 GHz. These results provide new opportunities to read out optical information in the THz domain. Furthermore, these compounds offer many prospects for optical switches, which can be performed by the so-called direct or reverse-LIESST effect (light-induced excited-spin state trapping). This phenomenon is attractive as it combines a low addressing power (about 5 mW/cm^2), a short addressing time (femtosecond scale, the spin transition being purely electronic in nature), a perfect reproducibility over successive cycles, even in a solid matrix and an optical reversibility, since the low-spin \rightarrow high-spin transition can be induced with a green light, while the reverse LS-HS state conversion can be addressed with a red light.

The authors thank K. Blary and all her colleagues for technical assistance at IEMN, Lille UMR CNRS 8520. J.F.L., A.K., and N.D. thank the Region Aquitaine and the Convention Renault-University Bordeaux 1 for the financial support.

- ¹See for general reviews, *Topics in Current Chemistry*, edited by P. Gütllich and H. A. Goodwin (Springer, New York, 2004).
- ²O. Kahn and C. Jay-Martinez, *Science* **279**, 5347 (1998).
- ³J.-F. Létard, P. Guionneau, and L. Goux-Capes, in *Topics in Current Chemistry*, edited by P. Gütllich and H. A. Goodwin (Springer, New York, 2004), Vol. 235, p. 221.
- ⁴R. N. Muller, L. V. Elst, and S. Laurent, *J. Am. Chem. Soc.* **125**, 8405 (2003).
- ⁵D. M. Mittleman, R. H. Jacobsen, and M. C. Nuss, *IEEE J. Quantum Electron.* **2**, 679 (1996).
- ⁶Q. Wu, T. D. Hewitt, and X. C. Zhang, *Appl. Phys. Lett.* **69**, 1026 (1996).
- ⁷B. M. Fischer, M. Walther, and P. Uhd Jepsen, *Phys. Med. Biol.* **21**, 3807 (2002).
- ⁸P. Haring Bolivar, M. Brucherseifer, M. Nagel, H. Kurz, A. Bosserhoff, and R. Tutner, *Phys. Med. Biol.* **21**, 3815 (2002).
- ⁹R. Sprik, I. N. Duling III, C. Chi, and D. Grischkowsky, *Appl. Phys. Lett.* **51**, 548 (1987).
- ¹⁰H. Nemeč, F. Kadlec, S. Surendran, P. Jungwirth, and P. Kuzel, *J. Chem. Phys.* **122**, 1 (2005).
- ¹¹H. Nemeč, F. Kadlec, S. Surendran, P. Jungwirth, and P. Kuzel, *J. Chem. Phys.* **122**, 12 (2005).
- ¹²C. A. Schmuttenmaer, G. M. Turner, and M. C. Beard, *Proc. SPIE* **5223**, 64 (2003).
- ¹³E. Freysz, S. Montant, S. Létard, and J.-F. Létard, *Chem. Phys. Lett.* **394**, 318 (2004).
- ¹⁴L. G. Lavrenova, V. N. Ikorskii, V. A. Varnek, I. M. Oglezneva, and S. V. Larionov, *Koord. Khim.* **16**, 654 (1990).
- ¹⁵P. Mounaix, M. Moustakim, S. Le Boiteux, J. P. Delville, R. Wunenburger, and L. Sarger, *Appl. Phys. Lett.* **83**, 5095 (2003).
- ¹⁶P. Mounaix, L. Sarger, J. P. Caumes, and E. Freysz, *Opt. Commun.* **242**, 631 (2004).
- ¹⁷C. Roman, O. Ichim, L. Sarger, P. Mounaix, and V. Vigneras, *Electron. Lett.* **40**, 1167 (2004).
- ¹⁸O. Kahn, J. Kröber, and C. Jay, *Adv. Mater. (Weinheim, Ger.)* **4**, 718 (1992).
- ¹⁹L. Duvillearet, F. Garet, and J. L. Coutaz, *IEEE J. Sel. Top. Quantum Electron.* **2**, 739 (1996).
- ²⁰M. Tondusson, L. Sarger, D. Michau, V. Reymond, M. Maglione, and P. Mounaix, *Jpn. J. Appl. Phys., Part 1* **44**, 5058 (2005).
- ²¹T. L. Chan, J. Bjarnason, J. E. W. M. Lee, M. A. Celis, and E. R. Brown, *Appl. Phys. Lett.* **85**, 2523 (2004).
- ²²A. Bousseksou, G. Molnar, P. Demont, and J. Menegotto, *J. Mater. Chem.* **13**, 2069 (2003).